Depletion of miR-96 Delays, But Does Not Arrest, Photoreceptor Development in Mice

Lue Xiang,[1,2] Juan Zhang,[1] Feng-Qin Rao,[1,3] Qiao-Li Yang,[1] Hui-Yi Zeng,[1] Sheng-Hai Huang,[1] Zhen-Xiang Xie,[1] Ji-Neng Lv,[1,2] Dan Lin,[1] Xue-Jiao Chen,[1,2] Kun-Chao Wu,[1] Fan Lu,[1,2] Xiu-Feng Huang,[4] and Qi Chen[1,2]

[1]School of Ophthalmology and Optometry, School of Biomedical Engineering, Eye Hospital, Wenzhou Medical University, Wenzhou, China
[2]State Key Laboratory of Ophthalmology, Optometry and Vision Science, Wenzhou, China
[3]School of Pharmaceutical Sciences of Wenzhou Medical University, Wenzhou, China
[4]The Second Affiliated Hospital of Wenzhou Medical University, Wenzhou, Zhejiang, China

Correspondence: Lue Xiang, School of Ophthalmology and Optometry, School of Biomedical Engineering, Eye Hospital, Wenzhou Medical University, Wenzhou 325027, China; xianglue324@foxmail.com.
Xiu-Feng Huang, The Second Affiliated Hospital of Wenzhou Medical University, Wenzhou, Zhejiang, China; hxfwzmc@163.com.
Qi Chen, School of Ophthalmology and Optometry, Institute of Biomedical Engineering, Eye Hospital, Wenzhou Medical University, Wenzhou 325027, China; qichen1983@126.com.

LX, JZ, and FQR contributed equally to this work.

Received: November 28, 2021
Accepted: April 10, 2022
Published: April 28, 2022

Citation: Xiang L, Zhang J, Rao FQ, et al. Depletion of miR-96 delays, but does not arrest, photoreceptor development in mice. *Invest Ophthalmol Vis Sci.* 2022;63(4):24. https://doi.org/10.1167/iovs.63.4.24

Purpose. Abundant retinal microRNA-183 cluster (miR-183C) has been reported to be a key player in photoreceptor development and functionality in mice. However, whether there is a protagonist in this cluster remains unclear. Here, we used a mutant mouse model to study the role of miR-96, a member of miR-183C, in photoreceptor development and functionality.

Methods. The mature miR-96 sequence was removed using the CRISPR/Cas9 genome-editing system. Electroretinogram (ERG) and optical coherence tomography (OCT) investigated the changes in structure and function in mouse retinas. Immunostaining determined the localization and morphology of the retinal cells. RNA sequencing was conducted to observe retinal transcription alterations.

Results. The miR-96 mutant mice exhibited cone developmental delay, as occurs in miR-183/96 double knockout mice. Immunostaining of cone-specific marker genes revealed cone nucleus mislocalization and exiguous Opn1mw/Opn1sw in the mutant (MT) mouse outer segments at postnatal day 10. Interestingly, this phenomenon could be relieved in the adult stages. Transcriptome analysis revealed activation of microtubule-, actin filament–, and cilia-related pathways, further supporting the findings. Based on ERG and OCT results at different ages, the MT mice displayed developmental delay not only in cones but also in rods. In addition, a group of miR-96 potential direct and indirect target genes was summarized for interpretation and further studies of miR-96–related retinal developmental defects.

Conclusions. Depletion of miR-96 delayed but did not arrest photoreceptor development in mice. This miRNA is indispensable for mouse photoreceptor maturation, especially for cones.

Keywords: miR-96, cone photoreceptor, development, gene regulation, dysfunction

In the human retina, cone photoreceptors are enriched in the macula and are responsible for keen visual acuity, providing sharp and colorful vision.[1] Cone cells differentiate from photoreceptor progenitors,[2,3] migrate to the macula,[4,5] and sense light with the aid of multiple opsins.[6,7] Harmful mutations in some proteins affecting the visual cycle and photoreceptor structures are suggested to result in early- and late-onset macular diseases, such as Stargardt disease and age-related macular degeneration.[8–10] Although a number of related coding genes have been reported and included in RetNet (https://sph.uth.edu/retnet),[11–20] the noncoding genes that influence the macula and cones have rarely been considered. miR-183C (composed of miR-182, miR-183, and miR-96) is abundantly expressed in human and animal retinas.[21–23] Triple and double knockout (KO) mouse models (miR-183/96) showed abnormal cone development,[24–27] which aroused our interest.

Actually, retinal miR-183C has attracted the attention of researchers in the past decade.[24–33] This cluster plays multiple roles in retinal development and homeostasis. It can act with environmental factors and may be responsible for some retinal diseases.[31–33] During development, disruption of miR-183C expression gives rise to cone maturation failure, heavily affecting electroretinogram (ERG) responses and inducing incorrect retinal lamination in mice.[24–30] Triple, double, or single knockout of the miRNAs in this cluster led to attenuated ERG responses, indicating an essential need for retinal homeostasis of miR-183C at the adult stage.[24,25,34,35] This versatile miR-183C cluster not only restricts its own functions in photoreceptors but also participates in immune

responses on the ocular surface and in retinal angiogenesis.[36–40] To be more precise, this cluster has impacts on the whole sensory system, including vision, hearing, pain, and taste.[25,41–48] Interestingly, this cluster can respond to light and may be involved in the eye–brain circadian rhythms of organisms.[31,49,50]

For the past several years, our group has had a great interest in uncovering the role of the individual miRNAs in miR-183C.[24,34,35] Among the sister miRNAs, miR-96 is expressed the least and is almost undetectable in retinal cone cells.[29] Mutations in the seed sequences cause hearing loss with unremarkable visual impairment in patients.[41,42] All of this information led us to study miR-182 and miR-183.[34,35] However, in this study, we sought to fully evaluate the remaining retinal miRNA, miR-96, in mice before we move forward to study the other noncoding regions in this cluster. Surprisingly, we found that miR-96 plays the most important role in cone development. Depleting this miRNA led to many cone nuclei remaining in the inner region of the outer nuclear layer (ONL) of developing mice at postnatal day (P) 10, similar to what occurs in miR-183/96 double KO (DKO) mice, in which cone migration from the inner region to the outer region is retarded.[24] In contrast to the DKO mice, most of the nuclei in the miR-96 mutant (MT) mice had reached the outer regions, as occurs in the wild-type (WT) mice during normal development. In addition, this phenomenon of developmental delay occurred in rods as well. Follow-up structural and functional analyses showed that these mice had functional attenuation, indicating a cooperative working mode of these sister miRNAs in retinal homeostasis. Based on our results, we believe that the individual roles of the three miR-183C components are now better understood in the mouse retina.

Materials and Methods

Generation and Genotyping of miR-96 Precise Mutant Mice

The miR-96 MT mice were generated by CRISPR/Cas9-mediated genome editing technology in a C57BL/6J background. The mouse miR-96 gene (MiRBase: MI0000583) is located on chromosome 6. The flanking sequence 5′-ACCATCTGCTTGGCCGATTTTGG-3′ was used as an single-guide RNA (sgRNA) to target the mouse miR-96 mature sequences. The founders were genotyped by DNA sequencing and T7E1 analysis. A mouse line carrying a 64-bp deletion (TTTGGCACTAGCACATTTTTGCTTGTGTCTCTCCGCTGTGAGCAATCATGTGTAGTGCCAATAT) was selected and bred for the present study. Both mature miR-96-5p and mature miR-96-3p sequences were removed, and the other regions were not affected.

Primer pairs for PCR were designed to differentiate MT from WT mice. The forward primer sequence was 5′-GGTGAGGAGGGTTGCTAAACTGC-3′, and the reverse primer sequence was 5′-GTAGCAGAAGGCTAGACCCCAAAGAC-3′. Sanger sequencing was used to define WT (651-bp PCR products) and MT (715-bp PCR products) individuals. The heterozygotes showed double-peak sequencing outcomes. All of the MT mice (generations after F5) used in this study were homozygotes.

Animal Care and Use

All mice were handled and maintained in the animal facility of the School of Ophthalmology and Optometry at Wenzhou Medical University as authorized by the Institutional Animal Care and Use Committee of Wenzhou Medical University.[51,52] All animal experiments were performed in accordance with the ARVO Statement for the Use of Animals in Ophthalmic and Vision Research.

Fundus Photography and Fundus Fluorescein Angiography

Fundus photography (FP) and fundus fluorescein angiography (FFA) were conducted to survey the potential fundus and blood vessel defects in miR-96 mutant mice using a Micron IV retinal imaging system (Phoenix Research Laboratories, Bend, OR, USA). Tropicamide (0.5%) was used to dilate the mouse pupils for 5 minutes. Subsequently, mice were anesthetized with a liquid mixture of ketamine (80 mg/kg) and xylazine (16 mg/kg) by intraperitoneal injection. A drop of ofloxacin eye ointment (Dicolol, Shenyang, China) was applied to the corneal surface to keep it moist. After calming, the mice were faced toward the Micron IV camera to capture FP. After the FP experiment, the mice were injected with AK-FLUOR (Akorn, Lake Forest, IL) (fluorescein injection, USP), and a similar capturing procedure was used to collect fluorescent pictures (FFA experiment).

Immunohistochemistry and TUNEL Assay

The mouse eyeballs were excised as quickly as possible from the euthanized mice and fixed in 4% paraformaldehyde for 15 minutes. After removal of the cornea and lens, the eyecups were refixed in 4% paraformaldehyde for 20 minutes, followed by dehydration in 30% sucrose in PBS three times. Ultimately, they were embedded in SAKURA (Torrance, CA) Tissue-Tek O.C.T. Retinal sections (20 µm thick) were gathered and rinsed three times in 0.01 M PBS. The retinal tissues were blocked in 4% bovine serum albumin (blocking buffer) and 0.5% Triton X-100 for 2 hours at room temperature. To obtain specific immunostaining, section slides were incubated with the corresponding primary antibodies overnight at 4°C. For secondary antibody incubation, the diluted antibodies were used at room temperature for 1 hour. Primary antibodies and their dilutions were as follows: rabbit-anti-cone arrestin (1:200; Millipore AB15282, Darmstadt, Germany), rabbit-anti-Opn1sw/S-opsin (1: 200; Millipore AB5407), rabbit-anti-Opn1mw/M-opsin (1:200; Millipore AB5405), and rat-anti-glial fibrillary acidic protein (GFAP, 1:500; Invitrogen 13-0300, Waltham, MA). Secondary antibodies donkey anti-rabbit Alexa488 (1:200; Jackson, Jackson ImmunoResearch, West Grove, PA) and donkey anti-rat Alexa488 (1:200; Jackson) were employed in the experiments. Cell nuclei of the tissues were stained with 4′,6-diamidino-2-phenylindole (1:5000; Sigma-Aldrich, St. Louis, MO, USA). TUNEL in situ labeling was conducted using the One Step TUNEL Apoptosis Assay Kit (Beyotime Biotechnology, Shanghai, China) according to the manufacturer's protocol.[53] Finally, images of the immunostained retinas were captured using a Zeiss confocal microscope (LSM880; Carl Zeiss Meditec, Jena, Germany).

Electroretinogram

miR-96 MT mice and age-matched WT controls were paired for the RETI-port ERG system (Ganzfeld Q450 SC; Roland Consult, Wiesbaden, Germany). Mice were dark-adapted for more than 2 hours and anesthetized with ketamine and

Investigative Ophthalmology & Visual Science

xylazine. Pupils were dilated, and gold wire loop electrodes were placed on both corneas. The mice were placed on a heating pad at 37°C to maintain the body temperature. Then, ERGs were performed according to the protocol described previously.[34] Only the values from the right eyes were included in the current study. The ERG parameters for photopic responses were used as follows: stimulation intensities at 0.48 log candela (cd)·s/m^2 (light 3.0). The ERG parameters for scotopic responses were used as follows: stimulation intensities at –2.02 log cd·s/m^2 (dark 0.01), 0.48 log cd·s/m^2 (dark 3.0), and 0.98 log cd·s/m^2 (dark 10.0).

RNA Isolation and Sequencing

Both eyeballs of miR-96 MT and WT mice were extirpated, and the retinas were isolated as soon as possible for total RNA extraction according to the instruction manual of Trizol Reagent (Life Technologies, Waltham, MA, USA). The cDNA library was constructed following the manufacturer's instructions of the NEBNext Ultra RNA Library Prep Kit for Illumina (NEB, E7530, Ipswich, MA) and NEBNext Multiplex Oligos for Illumina (NEB, E7500). Subsequently, the constructed cDNA libraries were sequenced on a flow cell using an Illumina NovaSeq 6000 platform. The RNA sequence (RNA-seq) data at P120 of miR-96 MT and WT retinas were accessible at the NCBI SRA repository with the accession numbers of SRR18217672, SRR18217673, SRR18217674, SRR18217675, SRR18217676, SRR18217677.

RNA-Seq Analyses

Gene expression levels were estimated using fragments per kilobase of exon per million fragments mapped (FPKM) values by Cufflinks software.[54] Differential gene expression between miR-96 MT and WT mice was evaluated by DESeq2 software.[55] Subsequently, gene abundance differences between those samples were calculated based on the ratio of the FPKM values. The false discovery rate (FDR) control method was used to account for multiple testing. Only genes with a fold change >1.2 and FDR significance score <0.05 were included for gene ontology (GO) analysis and KEGG (Kyoto Encyclopedia of Genes and Genomes) pathway analysis.

Optical Coherence Tomography Image Acquisition and Analysis

High-resolution spectral-domain optical coherence tomography (SD-OCT) (Spectralis HRA + OCT; Heidelberg Engineering, Heidelberg, Germany) with an 870-nm central wavelength and a 3.9-µm axial resolution was used to acquire intraretinal layer images of mice in the horizontal meridian centered on the optic nerve head. The mouse pupils were dilated with 0.5% tropicamide for 10 minutes, and then they were anesthetized with ketamine (80 mg/kg) and xylazine (16 mg/kg). One drop of Gen Teal lubricant eye gel (Novartis, East Hanover, NJ, USA) was administered to the eyes to keep the corneas moist. Then, the mice were positioned for SD-OCT image acquisition. A commercial ImageJ software program (version 1.53; National Institutes of Health, Bethesda, MD, USA) was used to manually outline the boundaries of the intraretinal layers (Supplementary Fig. S1), including the (1) internal limiting membrane (red line), (2) outer plexiform layer/ONL (blue line), (3) external limiting membrane (yellow line), (4) outer segment of photoreceptors (OS)/retinal pigment epithelium (RPE) (orange line), and (5) RPE/choroid (green line). The thicknesses of the whole retina and the intraretinal ONL and the combined inner segment (IS) and OS layers (i.e., IS/OS) were calculated by subtracting the boundary positions of each of the adjacent layers obtained by automated segmentation along with the depth based on MATLAB software (The MathWorks, Natick, MA, USA).

Statistical Analyses

The results were presented as the means ± SEMs, and statistical significance was assessed using two-tailed Student's *t*-tests. Statistical results were visualized using GraphPad Prism (GraphPad Software, La Jolla, CA, USA). Statistical significance was indicated as $^{*}P < 0.05$, $^{**}P < 0.01$, and $^{***}P < 0.001$ between the MT and WT groups.

Results

Depletion of the Mature miR-96 Sequences in Mice

A mouse model carrying a point mutation in the miR-96 seed sequence has been widely used in hearing research since 2009.[42,56–58] However, mouse models targeting the mature sequence of miR-96 for vision research are lacking. To obtain a miR-96–specific mutant mouse model, we designed a sgRNA to target the region near the seed sequence of miR-96 (Fig. 1A). With the help of the CRISPR/Cas9 gene-editing system, we finally obtained two strains. Luckily, one of the strains containing a 64-bp depletion with mature miR-96-5p, and the mature miR-96-3p sequence was perfectly removed (Figs. 1A, 1B). Because this strain precisely deleted the mature region without affecting other sequences, we chose to use it in our current research.

Developmental Delay of Cone Photoreceptors in miR-96 MT Mice

During WT mouse cone photoreceptor development, beginning at developmental stage P6, the nuclei of the cone cells spontaneously migrate to the outer region of the ONL.[24,25] By P30, almost all of the nuclei will become evenly arranged in the outer region. A typical phenotypic defect in cone nucleus polarization (retracted to the inner region of the ONL) in miR-183C KO models was highlighted in previous studies.[24,25] Hence, we performed similar immunostaining experiments for cone arrestin and M/S-opsin to determine if a single KO of miR-96 could replicate the phenotype, as we observed in miR-183/96 DKO mice.[24] Surprisingly, 43.6% of the cone nuclei had retracted to the inner region of the ONL in miR-96 MT mice at P10 (Figs. 2A, 2C). This percentage was very close to the 53.6% observed in DKO mice, suggesting that miR-96 may act as a protagonist in this cluster in terms of cone nuclei migration at an early stage. Interestingly, this phenomenon was vastly relieved at P90 and P180 (Fig. 2A). We found zero to three abnormal cones in which the nuclei remained at the inner region of the ONL in most visual fields viewed by confocal microscopy in the P90 and P180 mice (Fig. 2, Supplementary Fig. S2). Immunostaining of M/S-opsin further verified these observations (Fig. 2B, Supplementary Fig. S2).

Investigative Ophthalmology & Visual Science

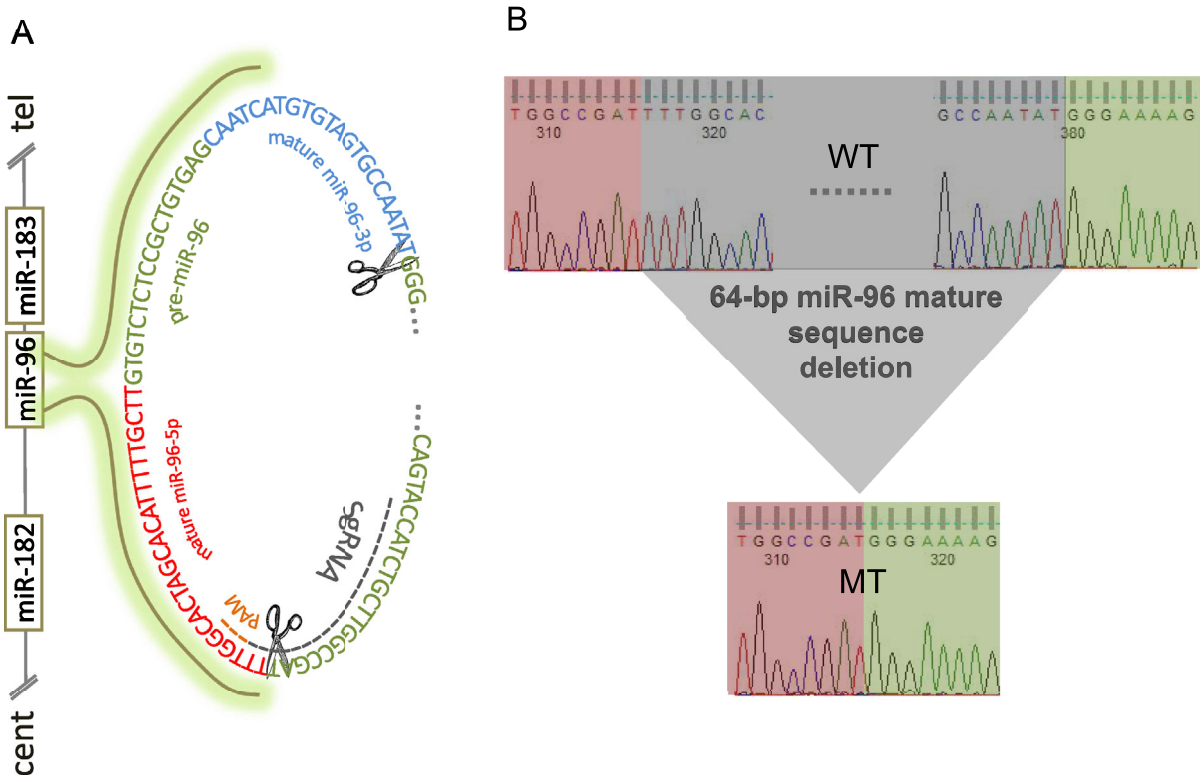

Figure 1. Precise depletion of mature miR-96 in mice. (**A**) Location of mouse miR-96 on chromosome 6. Single-guide RNAs (*gray*), PAM (*orange*), mature miR-96-5p (*red*), mature miR-96-3p (*blue*), and pre-miR-96 (*grayish green*) are labeled in the figure. (**B**) Genotyping strategy for the miR-96 MT and WT mice by DNA sequencing. The pairwise sequence comparison between WT and MT is shown. *Gray shade*, the 64-bp deletion includes the mature miR-96-5p and mature miR-96-3p of miR-96 MT mice. cent, centromeric; PAM, protospacer adjacent motif; tel, telomeric.

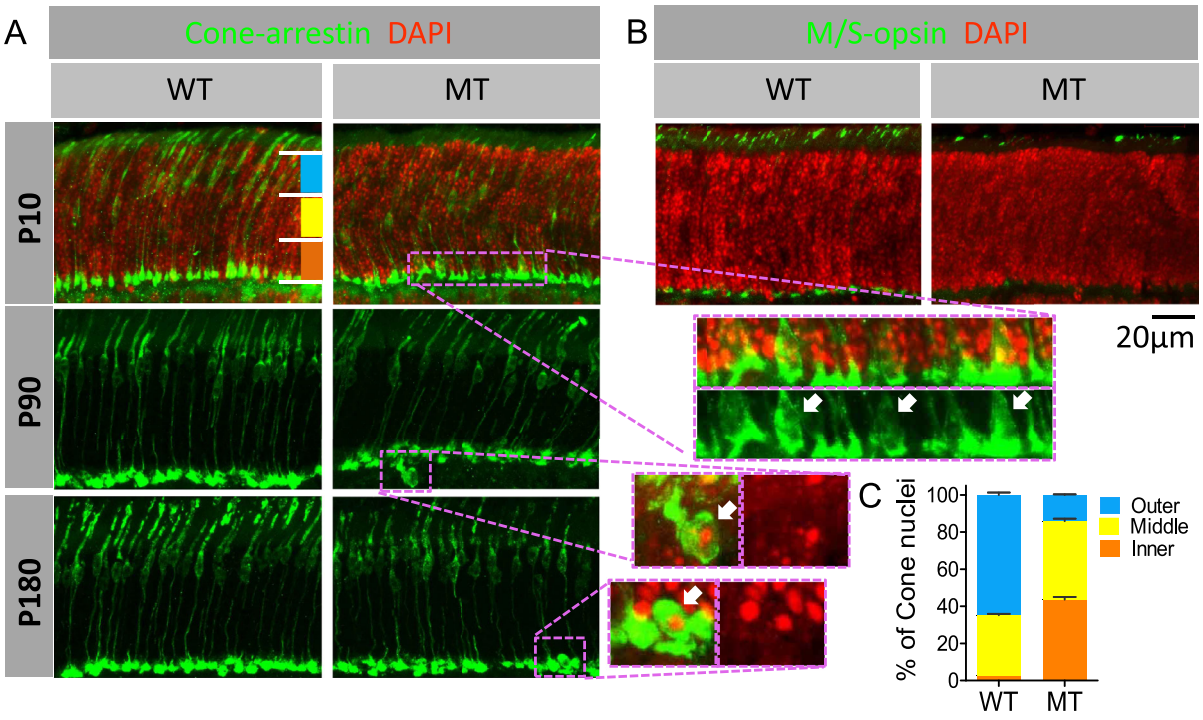

Figure 2. Depletion of miR-96 results in early-onset defects in cone nuclear polarization and shortened OSs in mice. (**A**) Immunostaining of cone arrestin at P10, P90, and P180 in WT (*left*) and miR-96 MT (*right*) mouse retinas. *White arrows* (*insets*) point to the location of cone nuclei at the inner region of the ONL. *Purple dotted areas* are magnified and shown as *inserts*. (**B**) Immunostaining of M/S-opsin at P10 in WT (*left*) and miR-96 MT (*right*) mouse retinas. *Scale bar*: 20 μm. (**C**) Quantification of cone nuclei of the ONL on the inner, middle, and outer areas shown in **A** at P10; $n = 6$.

Investigative Ophthalmology & Visual Science

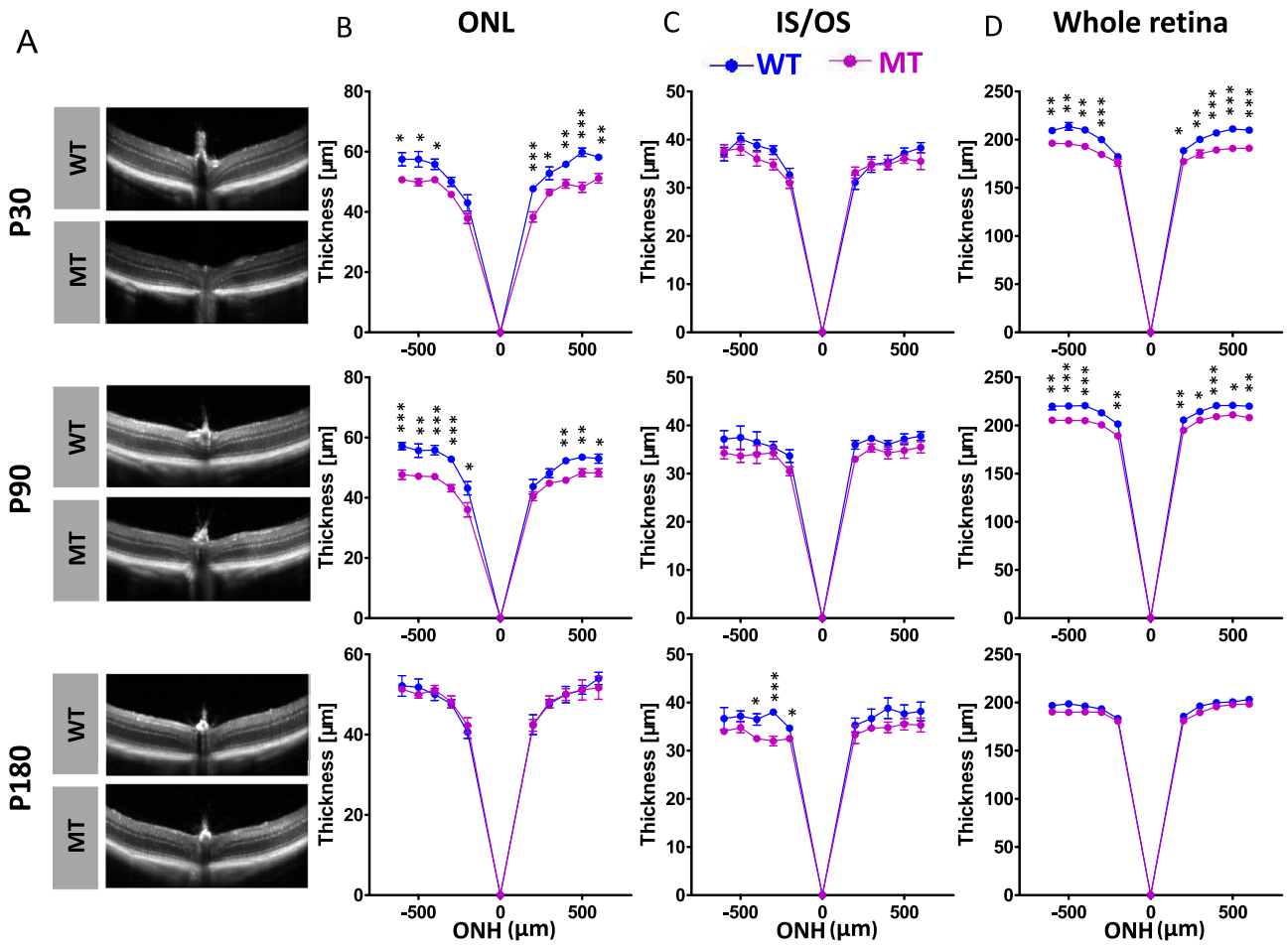

Figure 3. Retinal layer thicknesses in WT and miR-96 MT mice determined by SD-OCT. (**A**) Representative images of WT and miR-96 MT mice along the superior and inferior orientation at developmental stages P30, P90, and P180. *Scale bars*: 100 µm. (**B–D**) Measurements of the thicknesses of the whole retina, OS/IS, and ONL from the OCT images of mice at (**B**) P30, (**C**) P90, and (**D**) P180. The values are presented as means ± SEMs. $^{*}P < 0.05$, $^{**}P < 0.01$, $^{***}P < 0.001$, Student's *t*-test. $n = 6$ for each group. ONH, optic nerve head.

Developmental Delay of Rod Photoreceptors in miR-96 MT Mice

The delayed developmental feature was manifested not only in the cones but also in the rods (Fig. 3). Based on the analysis of ONL thickness determined by SD-OCT, the photoreceptor layer was significantly thinned in the miR-96 MT mice at P30 and P90, but there were no obvious changes in thickness at P180 (Figs. 3A, 3B). Because the ONL consists mostly of rods, this result indicated that the developmental delay of rods was evident in the mutants. Consistently, the differences in ONLs between WT and MT mice were reflected in the thicknesses of the whole retina (Figs. 3A, 3D). However, we observed no significant thickness change in IS/OS layers between these two groups (Fig. 3C). In addition to developmental delay, we carried out immunostaining of GFAP, a marker of retinal degeneration, and a TUNEL assay, a marker of apoptosis, in the miR-96 MT retinas from P10 to P180 (Supplementary Fig. S3). Interestingly, for these markers of cell degeneration, we did not observe a significant difference between the WT and MT groups. Negative results from these experiments indicated that progressive degeneration and cell loss did not occur in the miR-96 MT retinas. In summary, depletion of miR-96 resulted in photoreceptor developmental delay in mice.

Depletion of miR-96 Results in Recoverable ERG Responses in Developing Mice

To further analyze the functional changes in miR-96 MT mice, we recorded ERG responses at P30, P90, and P180 (Fig. 4). The photopic and scotopic b-wave responses in the MT retinas tended to be lower than in the WT retinas, but the differences were significant only for the photopic responses at P30 and P90 (Figs. 4A–D), and the scotopic response at P90 (Fig. 4E). None of the differences at P180 were significant. Thus, deletion of miR-96 reduced the ERG function of the photoreceptors at P30 and P90, but it recovered to WT levels by P180 (Figs. 4B, 4C, 4E, 4F). Overall, it showed "catch-up" growth in rod function, according to the changing percentages from P30 to P180 (dark 3.0: P30, 89.61%; P90, 56.68%; P180, 89.17% and dark 10.0: P30, 87.87%; P90, 65.99%; P180, 92.44%). Overall, the general trend of the

Investigative Ophthalmology & Visual Science

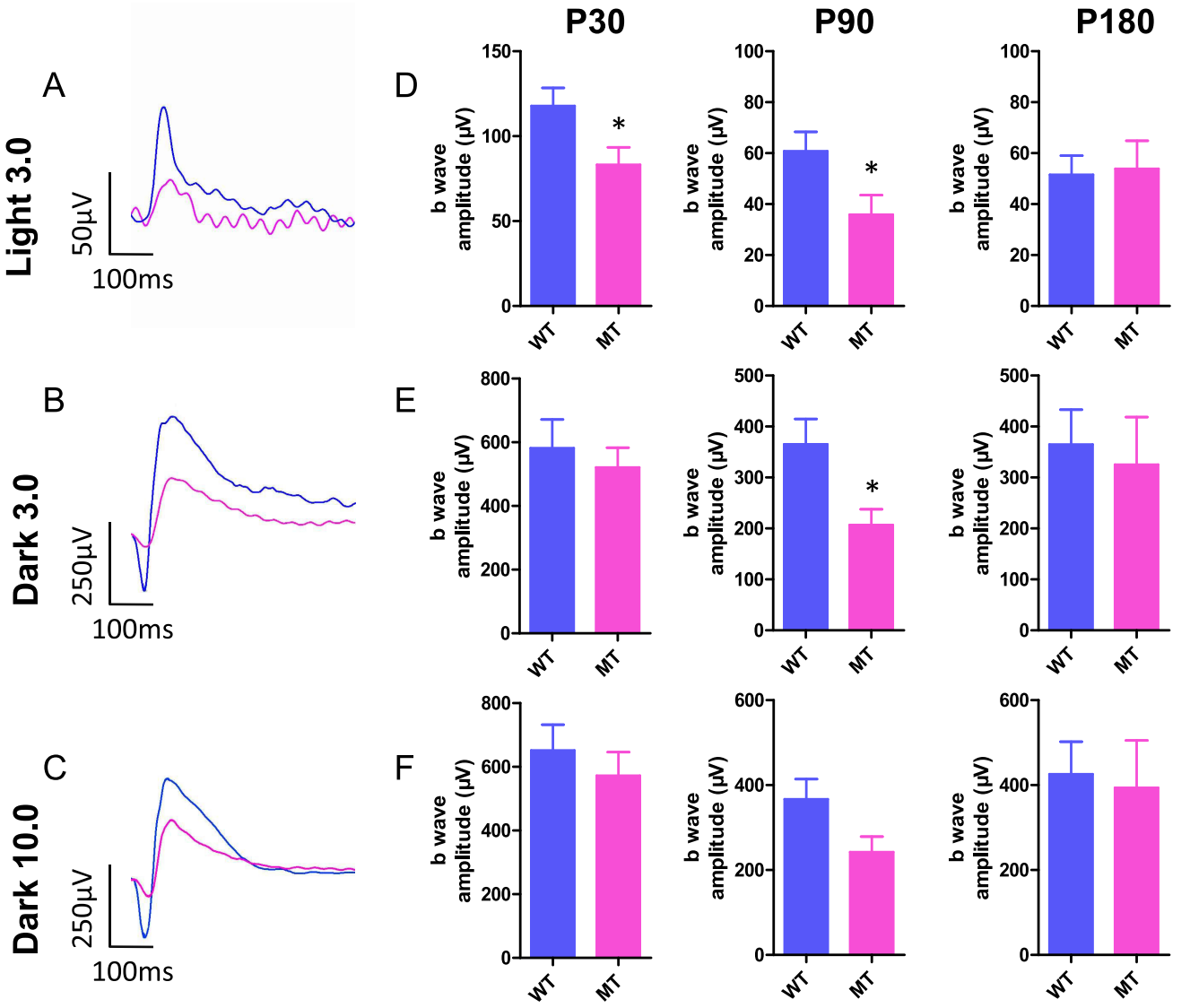

Figure 4. Evaluation of retinal function in miR-96 MT mice at P30, P90, and P180. (**A–C**) Representative ERG waves at (**A**) light 3.0, (**B**) dark 3.0, and (**C**) dark 10.0 at P90. (**D–F**) Statistical analysis of b-wave amplitudes at (**D**) light 3.0, (**E**) dark 3.0, and (**F**) dark 10.0. $n = 6$. *Error bars* represent SEM. *$P < 0.05$.

amplitude changes in the b-waves was also present in the a-waves (Supplementary Figs. S4A–C). However, none of the differences between the WT and MT retinas were statistically significant (Supplementary Figs. S4A–C).

Misexpression of Key Retinal Genes in miR-96 MT Mice

To identify which genes in the retina were affected by the depletion of miR-96, a whole-retina RNA-seq analysis was conducted at P120. In total, 430 differentially expressed genes (DEGs, fold change >1.2, FDR <0.05) were identified between the miR-96 MT mice and WT mice. These included 231 upregulated genes and 199 downregulated genes (Fig. 5A and Supplementary Excel). Among the 231 upregulated genes, 30 were candidate target genes (computationally analyzed using "TargetScan," http://www.targetscan.org/vert_80/) of miR-96 (Fig. 5B, Supplementary Table S1). Of note, mutations in the CERKL gene in humans led to cone rod dystrophy.[59,60] Interestingly, 13 genes of the 430 DEGs were linked to inherited retinal diseases in humans (RetNet database, https://sph.uth.edu/retnet/), including Adam9, Adipor1, Bbs4, Cerkl, Efemp1, Fscn2, Grk1, Guca1a, Mfsd8, Opn1mw, Pde6a, Sag, and Vcan. In addition to these causative genes of inherited retinal diseases, a few genes that have important roles in retinal function were also identified, such as Rims2 and Hcn1.

Based on the GO enrichment analysis, the top items of the biological process category were identified (Fig. 6). The retinoic acid receptor signaling pathway (GO:0048384) and embryonic eye morphogenesis (GO:0048048) were also identified in the analysis. These findings collectively suggest that deletion of miR-96 can lead to changes in the expression of key retinal genes and consequently may influence the retinal function.

Investigative Ophthalmology & Visual Science

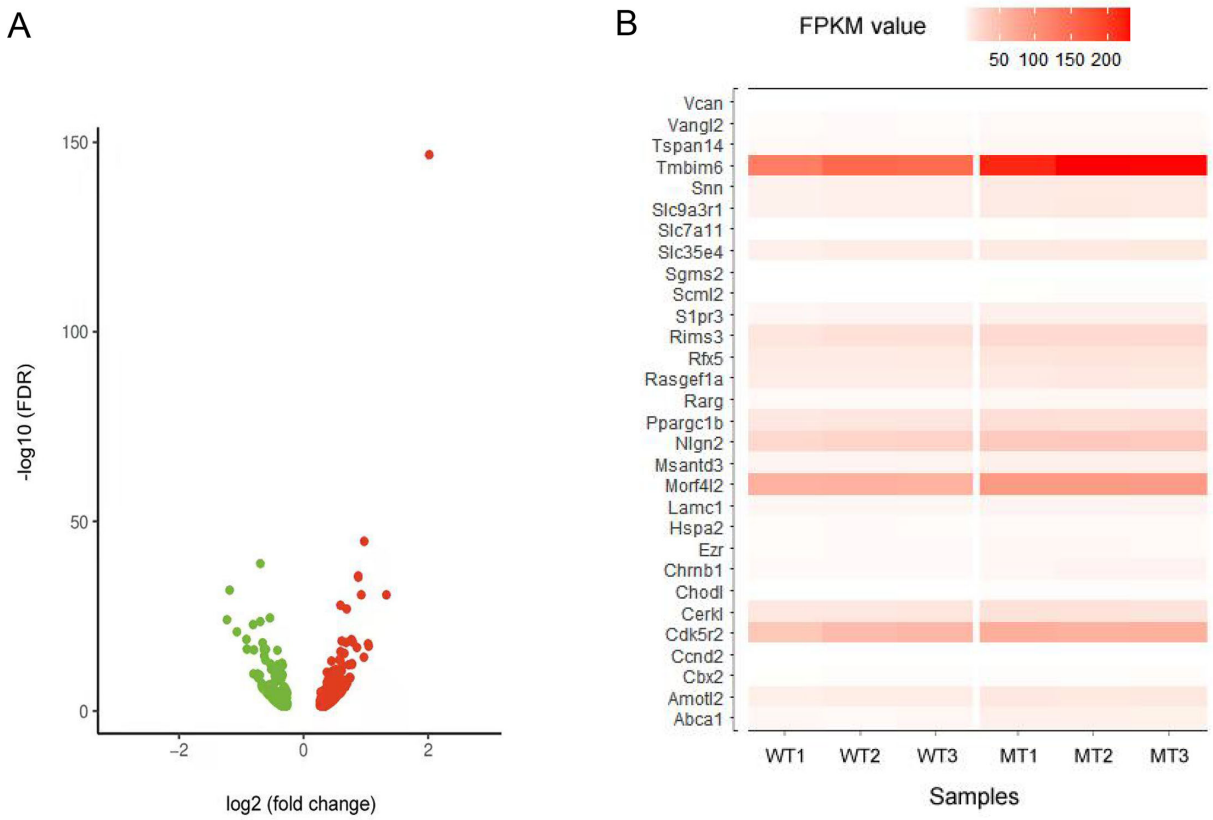

Figure 5. RNA sequencing and transcriptome analyses in mouse retinas. (**A**) Retinal DEGs between the miR-96 MT and WT mice. The upregulated genes are indicated with *red dots*, and the downregulated genes are indicated with *green dots*. (**B**) Heatmap of 30 differentially expressed genes that are potential targets of miR-96.

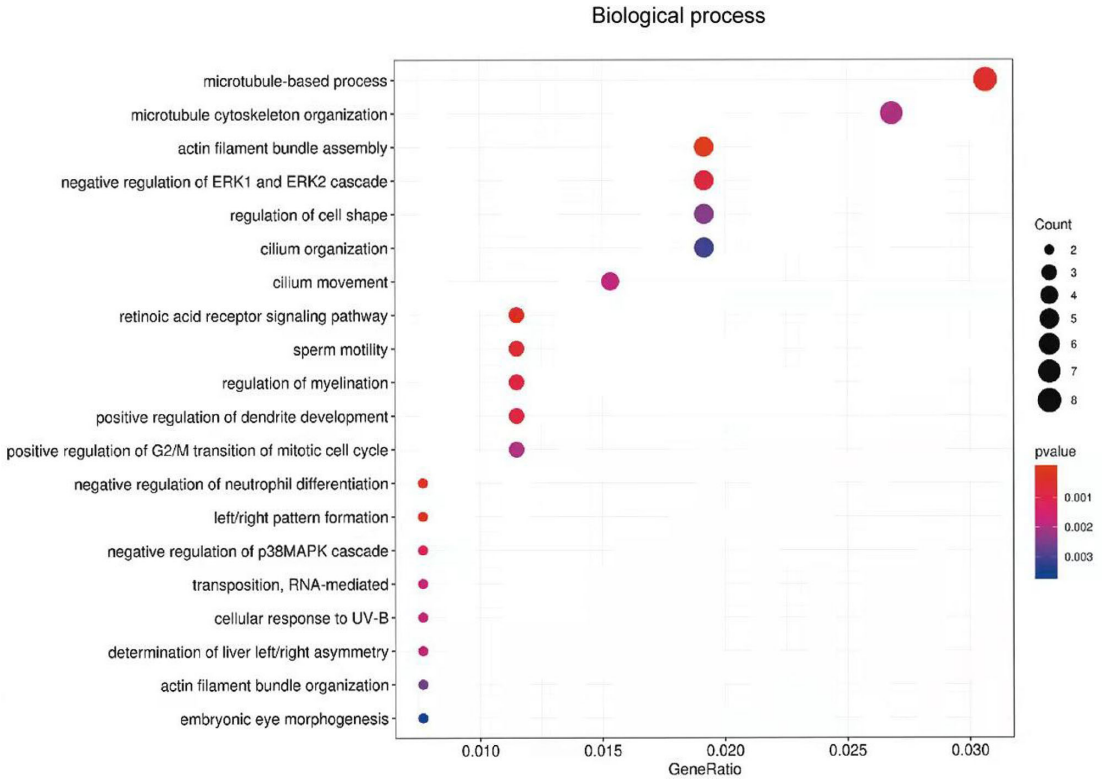

Figure 6. Biological process analysis. The *circle size* represents the gene count number, and the *red–blue gradient color bar* shows the *P* values of BP items. The most significant BP is ranked at the top. BP, biological process.

Investigative Ophthalmology & Visual Science

Transcriptome Alterations in miR-96 MT Retinas Support Photoreceptor Developmental Delay

Cell migration or polarization is not uncommon during the maturation of the neuronal system.[61–63] Cilia dynamics, actin filament dynamics, and microtubule formation are essential for this movement.[64–68] Interestingly, the GO enrichment analysis showed that multiple microtubule-related and cilia-related GO items were affected in miR-96 MT retinas, including microtubule-based processes (GO:0007017), microtubule cytoskeleton organization processes (GO:0000226), actin filament bundle assembly (GO:0051017), cilium organization (GO:0044782), and cilium movement (GO:0003341).

Moreover, there was an upregulation of several canonical retinal progenitor cell markers (e.g., Ccnd1, Ccnd2, Btg2)[69–72] and a downregulation of several crucial epigenetic regulators during retinal development (e.g., Ezh2 and Samd7)[73–77] in the P120 miR-96 MT retinas (Fig. 5 and Supplementary Excel). Taken together, the observations of gene expression alterations and GO item activations support the observed photoreceptor developmental delay in miR-96 MT mice, especially for cone photoreceptors.

Discussion

Our group has spent much effort characterizing the separate roles of the miRNAs in miR-183C.[24,34,35] Double knockout of miR-183/96 or triple knockout of the whole cluster results in severe retinal structural and functional alterations.[24,25] Single knockout of miR-182 and miR-183 impaired only the functionality of the retina without manifesting remarkable retinal architectural changes, such as cone nucleus mislocations during development.[34,35] Conversely, in our present study, we found significant architectural changes and mild functional alterations in developing miR-96 MT mice. Based on the aforementioned comprehensive data, we strongly speculate that miR-96 may cooperate with the other two members, miR-182 and miR-183, to control the morphogenesis and functionality of photoreceptors in mice.

Beginning at P10, the miR-96 MT mice had developmental defects in cones similar to miR-183/96 DKO mice.[24,25] Unlike the DKO mice, most of the cones gradually developed to the mature state without the aid of miR-96. These results suggest that the other noncoding regions of miR-183C (e.g., the intronic regions and the pre-miRNA sequences) are likely to play roles that promote cone photoreceptor correct localization apart from miR-96.[25] In our current study, we focused only on the developmental aspects of the miR-96 MT model without performing a long-term follow-up study for 1 or 2 years. Although no obvious changes were found in young mouse FP and FFA images (Supplementary Fig. S5), we cannot rule out a potential impact of miR-96 in aged mice.

In our current study, we obtained high-quality retinal transcriptome data that implicated multiple biological processes of cilia-related items and polarization-related items that could explain the defects causing the cone developmental delay. However, we do not know if there are some target genes of miR-96 that could also control or modulate the cone defects observed in the MT mice. miR-96 also targets Slc6a6 and Rnf217,[24,35] which were both increased in the MT group; however, they did not reach the criteria of "fold change >1.2, FDR < 0.05." This inconsistency may be due to the use of different candidate criteria (single target or cotarget) in different animal models.[24]

In hearing studies, miR-96 attracted the attention of researchers more than a decade ago.[41–44] Mutations in the seed sequences of miR-96 led to hearing loss in both animals and humans.[41–44] On the one hand, no obvious ophthalmologic impairments were found in deaf patients carrying mutations in miR-96.[41] On the other hand, our present miR-96 MT model displayed mild functional alterations and reversible photoreceptor developmental defects. Hence, we reasoned that deaf patients might have minor vision impairments at a level that could be easily neglected. Increasing the sample size, controlling the inclusion conditions, and paying more attention to retinal function tests may help address whether or not deaf patients carrying miR-96 should pay attention to vision loss. To date, except for miR-96, there have been few reports about miR-182 and miR-183, which are related to human hearing loss. A pain research team revealed that a single knockout of miR-96 or the whole cluster gives rise to abnormal pain perceptions.[45,46] Certainly, these evidences suggest the importance of miR-96 in sensory systems.

Our results show that depletion of miR-96 delayed but did not arrest cone development in mice, suggesting that this miRNA is a major factor for cone nucleus polarization in miR-183C. In general, miR-96 is indispensable for the maturation of photoreceptors in mice. Our work will provide great insights for future miR-96–related basic and clinical studies.

Acknowledgments

The authors thank Zhi-Li Zheng for the assistance of statistical analysis and Britt Bromberg of Xenofile Editing (www.xenofileediting.com) for providing language editing services for this manuscript. In addition, the authors thank the Specific Pathogen Free (SPF) animal facility at Wenzhou Medical University for supporting this project.

Supported by the National Natural Science Foundation of China (81800857, 31771390, 81870690), Zhejiang Provincial Natural Science Foundation of China (LY19H120003, LGD22H120001, LQ21H180011), and the program of Wenzhou Science and Technology Bureau of China (Y20211159).

Disclosure: **L. Xiang**, None; **J. Zhang**, None; **F.-Q. Rao**, None; **Q.-L. Yang**, None; **H.-Y. Zeng**, None; **S.-H. Huang**, None; **Z.-X. Xie**, None; **J.-N. Lv**, None; **D. Lin**, None; **X.-J. Chen**, None; **K.-C. Wu**, None; **F. Lu**, None; **X.-F. Huang**, None; **Q. Chen**, None

References

1. Thoreson WB, Dacey DM. Diverse cell types, circuits, and mechanisms for color vision in the vertebrate retina. *Physiol Rev*. 2019;99:1527–1573.
2. Chen S, Wang Q-L, Nie Z, et al. Crx, a novel Otx-like paired-homeodomain protein, binds to and transactivates photoreceptor cell-specific genes. *Neuron*. 1997;19:1017–1030.
3. Peng G-H, Chen S. Active opsin loci adopt intrachromosomal loops that depend on the photoreceptor transcription factor network. *Proc Natl Acad Sci USA*. 2011;108:17821–17826.
4. Springer AD. New role for the primate fovea: a retinal excavation determines photoreceptor deployment and shape. *Vis Neurosci*. 1999;16:629–636.
5. Bringmann A, Syrbe S, Görner K, et al. The primate fovea: structure, function and development. *Prog Retin Eye Res*. 2018;66:49–84.
6. Smallwood PM, Wang Y, Nathans J. Role of a locus control region in the mutually exclusive expression of human red

and green cone pigment genes. *Proc Natl Acad Sci USA*. 2002;99:1008–1011.
7. Smallwood PM, Ölveczky BP, Williams GL, et al. Genetically engineered mice with an additional class of cone photoreceptors: implications for the evolution of color vision. *Proc Natl Acad Sci USA*. 2003;100:11706–11711.
8. Rivera A, White K, Stöhr H, et al. A comprehensive survey of sequence variation in the ABCA4 (ABCR) gene in Stargardt disease and age-related macular degeneration. *Am J Hum Genet*. 2000;67:800–813.
9. Schultz DW, Klein ML, Humpert AJ, et al. Analysis of the ARMD1 locus: evidence that a mutation in HEMICENTIN-1 is associated with age-related macular degeneration in a large family. *Hum Mol Genet*. 2003;12:3315–3323.
10. Gold B, Merriam JE, Zernant J, et al. Variation in factor B (BF) and complement component 2 (C2) genes is associated with age-related macular degeneration. *Nat Genet*. 2006;38:458–462.
11. Botto C, Rucli M, Tekinsoy MD, Pulman J, Sahel J-A, Dalkara D. Early and late stage gene therapy interventions for inherited retinal degenerations. *Prog Retin Eye Res*. 2021;86:100975.
12. Hyttinen JM, Blasiak J, Felszeghy S, Kaarniranta K. MicroRNAs in the regulation of autophagy and their possible use in age-related macular degeneration therapy. *Ageing Res Rev*. 2021;67:101260.
13. Mitchell P, Liew G, Gopinath B, Wong TY. Age-related macular degeneration. *Lancet*. 2018;392:1147–1159.
14. Liu C, Nathans J. An essential role for frizzled 5 in mammalian ocular development. *Development*. 2008;135(21):3567–3576.
15. Veleri S, Manjunath SH, Fariss RN, et al. Ciliopathy-associated gene Cc2d2a promotes assembly of subdistal appendages on the mother centriole during cilia biogenesis. *Nat Commun*. 2014;5:1–12.
16. Chen X, Liu Y, Sheng X, et al. PRPF4 mutations cause autosomal dominant retinitis pigmentosa. *Hum Mol Genet*. 2014;23:2926–2939.
17. Yi Z, Ouyang J, Sun W, Li S, Xiao X, Zhang Q. Comparative exome sequencing reveals novel candidate genes for retinitis pigmentosa. *EBioMedicine*. 2020;56:102792.
18. Vijaysarathy C, Pasha SPBS, Sieving PA. Of men and mice: human X-linked retinoschisis and fidelity in mouse modeling. *Prog Retin Eye Res*. 2021;87:100999.
19. Ou J, Vijayasarathy C, Ziccardi L, et al. Synaptic pathology and therapeutic repair in adult retinoschisis mouse by AAV-RS1 transfer. *J Clin Invest*. 2015;125:2891–2903.
20. Koch SF, Duong JK, Hsu C-W, et al. Genetic rescue models refute nonautonomous rod cell death in retinitis pigmentosa. *Proc Natl Acad Sci USA*. 2017;114:5259–5264.
21. Xu S, Witmer PD, Lumayag S, Kovacs B, Valle D. MicroRNA (miRNA) transcriptome of mouse retina and identification of a sensory organ-specific miRNA cluster. *J Biol Chem*. 2007;282:25053–25066.
22. Lagos-Quintana M, Rauhut R, Meyer J, Borkhardt A, Tuschl T. New microRNAs from mouse and human. *RNA*. 2003;9:175–179.
23. Fishman ES, Louie M, Miltner AM, et al. MicroRNA signatures of the developing primate fovea. *Front Cell Dev Biol*. 2021;9:807.
24. Xiang L, Chen X-J, Wu K-C, et al. miR-183/96 plays a pivotal regulatory role in mouse photoreceptor maturation and maintenance. *Proc Natl Acad Sci USA*. 2017;114:6376–6381.
25. Fan J, Jia L, Li Y, et al. Maturation arrest in early postnatal sensory receptors by deletion of the miR-183/96/182 cluster in mouse. *Proc Natl Acad Sci USA*. 2017;114:E4271–E4280.
26. Zhu Q, Sun W, Okano K, et al. Sponge transgenic mouse model reveals important roles for the microRNA-183 (miR-183)/96/182 cluster in postmitotic photoreceptors of the retina. *J Biol Chem*. 2011;286:31749–31760.
27. Lumayag S, Haldin CE, Corbett NJ, et al. Inactivation of the microRNA-183/96/182 cluster results in syndromic retinal degeneration. *Proc Natl Acad Sci USA*. 2013;110:E507–E516.
28. Krol J, Krol I, Alvarez CPP, et al. A network comprising short and long noncoding RNAs and RNA helicase controls mouse retina architecture. *Nat Commun*. 2015;6:1–13.
29. Busskamp V, Krol J, Nelidova D, et al. miRNAs 182 and 183 are necessary to maintain adult cone photoreceptor outer segments and visual function. *Neuron*. 2014;83:586–600.
30. Loscher CJ, Hokamp K, Kenna PF, et al. Altered retinal microRNA expression profile in a mouse model of retinitis pigmentosa. *Genome Biol*. 2007;8:1–12.
31. Krol J, Busskamp V, Markiewicz I, et al. Characterizing light-regulated retinal microRNAs reveals rapid turnover as a common property of neuronal microRNAs. *Cell*. 2010;141:618–631.
32. Xu S, Coku A, Muraleedharan CK, et al. Mutation screening in the miR-183/96/182 cluster in patients with inherited retinal dystrophy. *Front Cell Dev Biol*. 2020;8:1680.
33. Huang X-F, Huang Z-Q, Fang X-L, Chen Z-J, Cheng W, Jin Z-B. Retinal miRNAs variations in a large cohort of inherited retinal disease. *Ophthalmic Genet*. 2018;39:175–179.
34. Wu K-C, Chen X-J, Jin G-H, et al. Deletion of miR-182 leads to retinal dysfunction in mice. *Invest Ophthalmol Vis Sci*. 2019;60:1265–1274.
35. Zhang C-J, Xiang L, Chen X-J, et al. Ablation of mature miR-183 leads to retinal dysfunction in mice. *Invest Ophthalmol Vis Sci*. 2020;61:12.
36. Muraleedharan CK, McClellan SA, Ekanayaka SA, et al. The miR-183/96/182 cluster regulates macrophage functions in response to *Pseudomonas aeruginosa*. *J Innate Immunity*. 2019;11:347–358.
37. Muraleedharan CK, McClellan SA, Barrett RP, et al. Inactivation of the miR-183/96/182 cluster decreases the severity of Pseudomonas aeruginosa-induced keratitis. *Invest Ophthalmol Vis Sci*. 2016;57:1506–1517.
38. Ichiyama K, Gonzalez-Martin A, Kim BS, et al. The microRNA-183-96-182 cluster promotes T helper 17 cell pathogenicity by negatively regulating transcription factor Foxo1 expression. *Immunity*. 2016;44:1284–1298.
39. Zhang Z-Z, Qin X-H, Zhang J. MicroRNA-183 inhibition exerts suppressive effects on diabetic retinopathy by inactivating BTG1-mediated PI3K/Akt/VEGF signaling pathway. *Am J Physiol Endocrinol Metab*. 2019;316:E1050–E1060.
40. Desjarlais M, Wirth M, Rivera JC, et al. MicroRNA-96 promotes vascular repair in oxygen-induced retinopathy—a novel uncovered vasoprotective function. *Front Pharmacol*. 2020;11:13.
41. Mencia A, Modamio-Høybjør S, Redshaw N, et al. Mutations in the seed region of human miR-96 are responsible for nonsyndromic progressive hearing loss. *Nat Genet*. 2009;41:609–613.
42. Lewis MA, Quint E, Glazier AM, et al. An ENU-induced mutation of miR-96 associated with progressive hearing loss in mice. *Nat Genet*. 2009;41:614–618.
43. Van den Ackerveken P, Mounier A, Huyghe A, et al. The miR-183/ItgA3 axis is a key regulator of prosensory area during early inner ear development. *Cell Death Differ*. 2017;24:2054–2065.
44. Li H, Kloosterman W, Fekete DM. MicroRNA-183 family members regulate sensorineural fates in the inner ear. *J Neurosci*. 2010;30:3254–3263.
45. Peng C, Li L, Zhang M-D, et al. miR-183 cluster scales mechanical pain sensitivity by regulating basal and neuropathic pain genes. *Science*. 2017;356:1168–1171.
46. Sun L, Xia R, Jiang J, et al. MicroRNA-96 is required to prevent allodynia by repressing voltage-gated sodium channels in spinal cord. *Prog Neurobiol*. 2021;202:102024.
47. Moore KB, Vetter ML. MicroRNA maintenance of cone outer segments. *Neuron*. 2014;83:510–512.

Investigative Ophthalmology & Visual Science

48. Banks SA, Pierce ML, Soukup GA. Sensational MicroRNAs: neurosensory roles of the MicroRNA-183 family. *Mol Neurobiol*. 2020;57:358–371.
49. Zhou L, Miller C, Miraglia LJ, et al. A genome-wide microRNA screen identifies the microRNA-183/96/182 cluster as a modulator of circadian rhythms. *Proc Natl Acad Sci USA*. 2021;118(1):e2020454118.
50. Ben-Moshe Z, Alon S, Mracek P, et al. The light-induced transcriptome of the zebrafish pineal gland reveals complex regulation of the circadian clockwork by light. *Nucleic Acids Res*. 2014;42:3750–3767.
51. Zhi Z, Xiang J, Fu Q, et al. The role of retinal connexins Cx36 and horizontal cell coupling in emmetropization in guinea pigs. *Invest Ophthalmol Vis Sci*. 2021;62:27.
52. Li H, Liu B, Lian L, et al. High dose expression of heme oxigenase-1 induces retinal degeneration through ER stress-related DDIT3. *Mol Neurodegener*. 2021;16:1–17.
53. Wu M-J, Deng Q-Q, Lei X-L, et al. Elavl2 regulates retinal function via modulating the differentiation of amacrine cells subtype. *Invest Ophthalmol Vis Sci*. 2021;62:1.
54. Trapnell C, Williams BA, Pertea G, et al. Transcript assembly and quantification by RNA-seq reveals unannotated transcripts and isoform switching during cell differentiation. *Nat Biotechnol*. 2010;28:511–515.
55. Love MI, Huber W, Anders S. Moderated estimation of fold change and dispersion for RNA-seq data with DESeq2. *Genome Biol*. 2014;15:550.
56. Chen J, Johnson SL, Lewis MA, et al. A reduction in Ptprq associated with specific features of the deafness phenotype of the miR-96 mutant mouse diminuendo. *Eur J Neurosci*. 2014;39:744–756.
57. Schlüter T, Berger C, Rosengauer E, et al. miR-96 is required for normal development of the auditory hindbrain. *Hum Mol Genet*. 2018;27:860–874.
58. Solda G, Robusto M, Primignani P, et al. A novel mutation within the MIR96 gene causes non-syndromic inherited hearing loss in an Italian family by altering pre-miRNA processing. *Hum Mol Genet*. 2012;21:577–585.
59. Aleman TS, Soumittra N, Cideciyan AV, et al. CERKL mutations cause an autosomal recessive cone-rod dystrophy with inner retinopathy. *Invest Ophthalmol Vis Sci*. 2009;50:5944–5954.
60. Littink KW, Koenekoop RK, van den Born LI, et al. Homozygosity mapping in patients with cone-rod dystrophy: novel mutations and clinical characterizations. *Invest Ophthalmol Vis Sci*. 2010;51:5943–5951.
61. Higginbotham H, Eom TY, Mariani LE, et al. Arl13b in primary cilia regulates the migration and placement of interneurons in the developing cerebral cortex. *Dev Cell*. 2012;23:925–938.
62. McClintock TS, Khan N, Xie C, Martens JR. Maturation of the olfactory sensory neuron and its cilia. *Chem Senses*. 2020;45:805–822.
63. Driver EC, Northrop A, Kelley MW. Cell migration, intercalation and growth regulate mammalian cochlear extension. *Development*. 2017;144:3766–3776.
64. Seetharaman S, Etienne-Manneville S. Cytoskeletal crosstalk in cell migration. *Trends Cell Biol*. 2020;30:720–735.
65. Xie X, Wang S, Li M, et al. alpha-TubK40me3 is required for neuronal polarization and migration by promoting microtubule formation. *Nat Commun*. 2021;12:4113.
66. Munoz-Estrada J, Ferland RJ. Ahi1 promotes Arl13b ciliary recruitment, regulates Arl13b stability and is required for normal cell migration. *J Cell Sci*. 2019;132(17):jcs230680.
67. Eom TY, Stanco A, Guo J, et al. Differential regulation of microtubule severing by APC underlies distinct patterns of projection neuron and interneuron migration. *Dev Cell*. 2014;31:677–689.
68. Guemez-Gamboa A, Coufal NG, Gleeson JG. Primary cilia in the developing and mature brain. *Neuron*. 2014;82:511–521.
69. Clark BS, Stein-O'Brien GL, Shiau F, et al. Single-cell RNA-seq analysis of retinal development identifies NFI factors as regulating mitotic exit and late-born cell specification. *Neuron*. 2019;102:1111–1126.e1115.
70. Wong L, Power N, Miles A, Tropepe V. Mutual antagonism of the paired-type homeobox genes, vsx2 and dmbx1, regulates retinal progenitor cell cycle exit upstream of ccnd1 expression. *Dev Biol*. 2015;402:216–228.
71. Farhy C, Elgart M, Shapira Z, et al. Pax6 is required for normal cell-cycle exit and the differentiation kinetics of retinal progenitor cells. *PLoS One*. 2013;8:e76489.
72. Lu Y, Shiau F, Yi W, et al. Single-cell analysis of human retina identifies evolutionarily conserved and species-specific mechanisms controlling development. *Dev Cell*. 2020;53:473–491.e479.
73. Corso-Diaz X, Jaeger C, Chaitankar V, Swaroop A. Epigenetic control of gene regulation during development and disease: a view from the retina. *Prog Retin Eye Res*. 2018;65:1–27.
74. Rao RC, Tchedre KT, Malik MT, et al. Dynamic patterns of histone lysine methylation in the developing retina. *Invest Ophthalmol Vis Sci*. 2010;51:6784–6792.
75. Omori Y, Kubo S, Kon T, et al. Samd7 is a cell type-specific PRC1 component essential for establishing retinal rod photoreceptor identity. *Proc Natl Acad Sci USA*. 2017;114:E8264–E8273.
76. Hlawatsch J, Karlstetter M, Aslanidis A, et al. Sterile alpha motif containing 7 (samd7) is a novel crx-regulated transcriptional repressor in the retina. *PLoS One*. 2013;8:e60633.
77. Duraisamy AJ, Mishra M, Kowluru RA. Crosstalk between histone and DNA methylation in regulation of retinal matrix metalloproteinase-9 in diabetes. *Invest Ophthalmol Vis Sci*. 2017;58:6440–6448.

Investigative Ophthalmology & Visual Science